The aryl hydrocarbon receptor links integrin signaling to the TGF- pathway

Silginer, M ; Burghardt, I ; Gramatzki, D ; Bunse, L ; Leske, H ; Rushing, E J ; Hao, N ; Platten, M ; Weller, M ; Roth, P

Abstract: Glioblastoma is the most common and aggressive form of intrinsic brain tumor. Transforming growth factor (TGF)- represents a central mediator of the malignant phenotype of these tumors by promoting invasiveness and angiogenesis, maintaining tumor cell stemness and inducing profound immunosuppression. Integrins, which are highly expressed in glioma cells, interact with the TGF- pathway. Furthermore, a link has been described between activity of the transcription factor aryl hydrocarbon receptor (AhR) and TGF- expression. Here we demonstrate that integrin inhibition, using v, 3 or 5 neutralizing antibodies, RNA interference-mediated integrin gene silencing or pharmacological inhibition by the cyclic RGD peptide EMD 121974 (cilengitide) or the non-peptidic molecule GLPG0187, inhibits AhR activity. These effects are independent of cell detachment or cell density. While AhR mRNA expression was not affected by integrin inhibition, AhR total and nuclear protein levels were reduced, suggesting that integrin inhibition-mediated regulation of AhR may occur at a post-transcriptional level. AhR-null astrocytes, AhR-null hepatocytes or glioblastoma cells with a transiently silenced AhR gene showed reduced sensitivity to integrin inhibition-mediated alterations in TGF- signaling, indicating that AhR mediates integrin control of the TGF- pathway. Accordingly, there was a significant correlation of v integrin levels with nuclear AhR and pSmad2 levels as determined by immunohistochemistry in human glioblastoma in vivo. In summary, this study identifies a signaling network comprising integrins, AhR and TGF- and validates integrin inhibition as a promising strategy not only to inhibit angiogenesis, but also to block AhR- and TGF- -controlled features of malignancy in human glioblastoma.Oncogene advance online publication, 26 October 2015; doi:10.1038/onc.2015.387.

DOI: https://doi.org/10.1038/onc.2015.387

The aryl hydrocarbon receptor links integrin signaling to the TGF-β pathway

Manuela Silginer[1], Isabel Burghardt[1], Dorothee Gramatzki[1], Lukas Bunse[2], Henning Leske[3], Elisabeth J. Rushing[3], Nan Hao[4], Michael Platten[2], Michael Weller[1], Patrick Roth[1]

[1]Laboratory of Molecular Neuro-Oncology, Department of Neurology, University Hospital Zurich and University of Zurich, Zurich, Switzerland; [2]Department of Neurology, University Hospital Heidelberg, National Center for Tumor Diseases and German Cancer Consortium (DKTK) Clinical Cooperation Unit Neuroimmunology and Brain Tumor Immunology, German Cancer Research Center (DKFZ), Heidelberg, Germany; [3]Institute of Neuropathology, University Hospital Zurich and University of Zurich, Zurich, Switzerland; [4]School of Biological Sciences, University of Adelaide, Adelaide, Australia.

Correspondence: Dr. Patrick Roth, Department of Neurology, University Hospital Zurich, Frauenklinikstrasse 26, 8091 Zurich, Switzerland, Tel.: +41 (0)44 255 5511, Fax: +41 (0)44 255 4507, E-mail: patrick.roth@usz.ch

Running title: The integrin-AhR-TGF-β axis in glioma cells

Abstract

Glioblastoma is the most common and aggressive form of intrinsic brain tumor. Transforming growth factor (TGF)-β represents a central mediator of the malignant phenotype of these tumors by promoting invasiveness and angiogenesis, maintaining tumor cell stemness, and inducing profound immunosuppression. Integrins, which are highly expressed in glioma cells, interact with the TGF-β pathway. Furthermore, a link has been described between activity of the transcription factor aryl hydrocarbon receptor (AhR) and TGF-β expression.

Here we demonstrate that integrin inhibition, using αv, β3 or β5 neutralizing antibodies, RNA interference-mediated integrin gene silencing or pharmacological inhibition by the cyclic RGD peptide EMD 121974 (cilengitide) or the non-peptidic molecule GLPG0187, inhibits AhR activity. These effects are independent of cell detachment or cell density. While AhR mRNA expression was not affected by integrin inhibition, AhR total and nuclear protein levels were reduced, suggesting that integrin inhibition-mediated regulation of AhR may occur at a posttranscriptional level. AhR-null astrocytes, AhR-null hepatocytes, or glioblastoma cells with a transiently silenced AhR gene showed reduced sensitivity to integrin inhibition-mediated alterations in TGF-β signaling indicating that AhR mediates integrin control of the TGF-β pathway. Accordingly, there was a significant correlation of αv integrin levels with nuclear AhR and pSmad2 levels as determined by immunohistochemistry in human glioblastoma *in vivo*.

In summary, this study identifies a signaling network comprising integrins, AhR and TGF-β and validates integrin inhibition as a promising strategy not only to inhibit angiogenesis, but also to block AhR- and TGF-β-controlled features of malignancy in human glioblastoma.

Keywords: glioma, integrin, AhR, TGF-β

Introduction

The aryl hydrocarbon receptor (AhR) belongs to the family of basic helix-loop-helix/Per/ARNT/Sim (PAS) transcription factors and is the only member known to be activated by a ligand. In addition to the over 400 exogenous ligands, among them polycyclic aromatic hydrocarbons (PAH) and dioxins, endogenous AhR ligands such as tryptophan derivatives have been identified (1, 2). In the absence of ligand, AhR is present in the cytoplasm, bound to several molecular chaperone proteins including heat shock protein 90 (HSP90), the AhR-interacting protein (AIP) and the co-chaperone p23, maintaining an inactive state. Ligand binding induces a conformational change of AhR, resulting in its nuclear translocation by release of the chaperone complex and heterodimerization with AhR nuclear translocator (ARNT). The AhR/ARNT complex binds to its binding motif, the dioxin responsive elements (DRE), present in the promoter of target genes like CYP1A1 that is coding for a xenobiotic-metabolizing enzyme (3). In addition to this canonical signaling, several non-canonical signaling pathways have been described for AhR such as its direct association with the hyperphosphorylated retinoblastoma protein (pRB) which induces G_1-cell cycle arrest or its action as a ligand-dependent E3 ubiquitin ligase mediating polyubiquitination (4). Beside its critical role in xenobiotic-induced toxicity and carcinogenesis, AhR regulates multiple processes such as cellular proliferation and differentiation, tumor development and progression as well as cell motility and migration under physiological conditions, too (5). Depending on the tumor type, AhR may exhibit tumor suppressive or oncogenic activity (6). Human gliomas produce kynurenine (Kyn), an endogenous ligand generated via tryptophan-2,3-dioxygenase (TDO), which activates the AhR pathway, thus leading to tumor progression and poor survival (7). Moreover, inhibition of AhR signaling results in reduced proliferation, clonogenicity, invasiveness and transforming growth factor (TGF)-β signaling in human glioma cell lines (8). TGF-β is a central mediator of the malignant phenotype of gliomas that promotes growth, invasiveness, angiogenesis as well as

stemness and contributes to the immune evasion of these tumors (9, 10). Recently, we have shown that inhibition of αv integrins reduces TGF-β expression and down-stream signaling (11). Integrins are cell surface receptors formed by the combination of 18 α and 8 β subunits that play important and diverse roles in many biological processes such as cell adhesion, migration, invasion, survival and angiogenesis. Moreover, certain integrins are overexpressed in tumor cells as well as tumor-associated host cells and may have a profound role in tumor progression (12). AhR in turn may regulate the composition of integrin receptors on the cell surface and signaling of focal adhesion kinase (FAK), a non-receptor protein tyrosine kinase involved in integrin signaling cascades (5, 13, 14). Here, we aimed at defining a possible interplay of integrins and AhR in the regulation of TGF-β signaling in glioblastoma.

Results

Integrin inhibition reduces AhR activity in human glioma cells

In order to analyze whether integrin inhibition interferes with AhR signaling, we first assessed a *bona fide* target of AhR, that is, CYP1A1 (15). LN-308 cells were transiently transfected with the CYP1A1 reporter construct (DRE). Pharmacological integrin inhibition using cilengitide or GLPG0187 significantly reduced DRE reporter activity in a concentration-dependent manner. The AhR receptor antagonist CH-223191 was used as a positive control (Fig. 1A,B). Similarly, exposure to antibodies neutralizing different αv integrins decreased DRE reporter activity confirming the assumption that integrin inhibition interferes with AhR activity (Fig. 1C). These findings were further corroborated using RNA interference to specifically silence single αv-integrins. As shown before, exposure to integrin-specifc siRNA molecules resulted in reduced expression of the targeted integrin in LN-308 glioma cells (11). Integrin gene silencing was paralleled by a significant reduction of DRE reporter activity (Fig. 1D). Next we asked whether integrin inhibition-induced cell detachment interferes with AhR signaling (16). For this purpose, we separately analyzed the attached and floating fractions of LN-308 cells upon integrin inhibition. AhR signaling was reduced to a similar extent in both cell fractions, indicating that the observed effects occur independently of cell detachment. CH-223191 and the AhR agonist 3-methylcholanthrene (3-MC) were used as controls (Fig. 1E). Moreover, LN-229 cells, which do not detach or die upon integrin inhibition (16), also displayed reduced DRE reporter activity in response to integrin inhibition (Fig. 1F). To further confirm the hypothesis that integrin inhibition interferes with AhR signaling, mRNA levels of the AhR-responsive gene, CYP1A1, were determined. Pharmacological integrin inhibition resulted in strongly reduced CYP1A1 mRNA levels while exposure to CH-223191 or 3-MC reduced or increased CYP1A1 mRNA expression, respectively (Fig. 1G). Time course analyses demonstrated a reduction of CYP1A1 mRNA levels

within 48 h following integrin inhibition (Fig. 1H). In line with these findings, a dramatic reduction of CYP1A1 expression levels was observed when cells were treated with specific anti-αv integrin antibodies (Fig. 1I). Additionally, integrin gene silencing by RNA interference reduced the expression of CYP1A1, confirming the link between integrin signaling and AhR expression (Fig. 1J).

Because of their potential contribution to therapy resistance, we assessed the interaction between integrins and AhR activity in a panel of GIC lines, too. Interference with integrin signaling using the pharmacological inhibitors cilengitide (Fig. 2A) or GLPG0187 (Fig. 2B) resulted in reduced DRE reporter activity in GIC lines. Moreover, the expression of the AhR target gene CYP1A1 was reduced (Fig. 2C). Accordingly, the integrin-AhR axis is also present in the population of glioma cells with stem cell properties.

Inhibition of integrin activity reduces AhR protein levels

Next we addressed the mechanism mediating reduced AhR signaling upon integrin inhibition. Integrin inhibition using pharmacological inhibitors or specific siRNA oligonucleotides did not alter levels of AhR transcripts (Fig. 3A). Plasmid-mediated gene transfer was used to express a constitutive active form of AhR (AhR-CA) in LN-229 cells. Here, the expression of AhR is controlled by an independent promoter. Upon exposure of LN-229 control or AhR-CA cells to control peptide or cilengitide, DRE reporter activity was determined. Integrin inhibition decreased AhR reporter activity not only in control, but also in AhR-CA cells, confirming that altered AhR signaling upon integrin inhibition is not mediated by transcriptional regulation (Fig. 3B, top). Moreover, while AhR-CA cells expressed higher mRNA levels of the target gene CYP1A1 than control cells, integrin inhibition reduced CYP1A1 expression in both cell lines (Fig. 3B, bottom). However, when we analyzed AhR protein expression upon integrin inhibition using cilengitide, we found a reduction in a concentration-dependent manner. Parallel activity on the TGF-β pathway activity was confirmed at the level of Smad2 phosphorylation (Fig. 3C). Moreover, we

specifically asked whether integrin inhibition interferes with AhR activation, that is, translocation and nuclear accumulation of AhR, too. To this end, fractionated lysates of LN-308 cells exposed to the control peptide RAD (cyclo-(Arg-Ala-Asp-DPhe-Val)) or cilengitide were prepared to determine AhR nuclear and cytoplasmic protein levels separately. Integrin inhibition strongly reduced nuclear AhR levels whereas the cytoplasmic levels of AhR remained unaltered (Fig. 3D). To support these findings, we examined glioma cells by immunofluorescence for AhR following integrin inhibition. Here, cilengitide diminished total AhR as well as nuclear AhR levels (Fig. 3E) confirming the influence of integrin activity on AhR protein levels.

Integrin-mediated control of the TGF-β pathway is abrogated by AhR gene silencing

Based on the findings that integrin inhibition interferes with TGF-β signaling (11) and that AhR controls the TGF-β pathway in human glioma cells (8), we asked whether integrin inhibition-mediated effects on TGF-β signaling are promoted by AhR. Hence, we analyzed murine $AhR^{+/+}$ (control) and $AhR^{-/-}$ (AhR-null) hepatocytes that had been isolated from wild-type or AhR-KO mice (17), for alterations in the TGF-β pathway upon integrin inhibition. Absence of AhR mRNA expression in $AhR^{-/-}$ cells was confirmed by real-time PCR (Fig. 4A, top). mRNA levels of the AhR response gene CYP1A1 were reduced compared to control cells. Moreover, exposure to cilengitide resulted in reduced CYP1A1 mRNA expression only in $AhR^{+/+}$ hepatocytes, suggesting that this effect is AhR-mediated (Fig. 4A, bottom). Furthermore, integrin inhibition resulted in a reduction of DRE reporter activity in control, but not in $AhR^{-/-}$ hepatocytes (Fig. 4B). Finally, immunoblot analysis demonstrated that constitutive pSmad2 protein levels were similar in control and AhR-null hepatocytes. However, integrin inhibition reduced Smad2 phosphorylation more efficiently in control cells than in AhR-null hepatocytes, indicating that AhR contributes to integrin inhibition-mediated effects on the TGF-β pathway (Fig. 4C). Based on the finding that murine hepatocytes detached and died upon integrin inhibition (data not shown) and previous work demonstrating that detachment may also affect TGF-β signaling (11, 18), we

extended our investigations to human HaCaT keratinocytes, with lentivirus-mediated AhR silencing, which neither detached nor died upon integrin inhibition (data not shown). Compared to control cells, AhR and CYP1A1 mRNA levels were strongly diminished in AhR-deficient keratinocytes. Integrin inhibition had no effect on AhR mRNA expression in control or AhRsi cells and a significant loss in CYP1A1 levels was detected in HaCaT control cells only (Fig. 5A). Expectedly, AhR protein levels were lower in AhRsi keratinocytes compared to control. Integrin inhibition resulted in reduced AhR protein levels in HaCaT control cells but no such effect was observed in HaCaT cells with silenced AhR (Fig. 5B, E). Moreover, integrin inhibition reduced DRE reporter activity in HaCaT control cells in a concentration-dependent manner, but not in AhRsi cells (Fig. 5C). Constitutive TGF-β_2 mRNA levels were lower in AhRsi than in control cells, suggesting that TGF-β_2 signaling is under control of AhR in these cells, thus making them an appropriate model to study the relevance of AhR for integrin inhibition-mediated interference with the TGF-β pathway. Cilengitide strongly reduced TGF-β_2 mRNA expression in HaCaT control, but not in AhRsi cells, whereas no effect on TGF-β_1 mRNA levels was detected (Fig. 5D). Accordingly, HaCaT AhRsi cells showed reduced constitutive expression of pSmad2, whereas integrin inhibition reduced pSmad2 levels only in HaCaT control, but not in AhRsi cells (Fig. 5E).

The integrin-AhR-TGF-β signaling axis is active in cells of glial origin

In order to investigate the relevance of the identified signaling axis in cells of glial origin, we next analyzed astrocytes obtained from AhR-null mice. Absence of AhR mRNA expression and a decrease of CYP1A1 mRNA expression were observed in AhR-null astrocytes relative to AhR-expressing astrocytes (control). Moreover, a significant reduction of CYP1A1 expression upon integrin inhibition was detected only in control cells (Fig. 6A, top, middle). Again, compared with control cells, TGF-β_2 mRNA levels were lower and sensitivity to cilengitide was lacking in AhR-null astrocytes (Fig. 6A, bottom). TGF-β_1 expression levels were at the detection limit in these cells (data not shown). Finally, to proof our hypothesis in glioblastoma cells, we transiently

silenced AhR in LN-308 cells using RNA interference which resulted in strongly reduced AhR mRNA levels. Integrin inhibition did not alter AhR expression, whereas a trend towards reduced CYP1A1 mRNA levels was observed in control and AhRsi cells (Fig. 6B). Besides, cilengitide reduced AhR protein levels and DRE reporter activity in control, but not in AhRsi cells (Fig. 6C). Constitutive TGF-β_2 mRNA expression was reduced in AhRsi cells compared to control cells and cilengitide strongly reduced TGF-β_2 mRNA expression in control cells only. Again, TGF-β_1 mRNA levels were not affected by AhR knockdown nor by integrin inhibition, suggesting that control of TGF-β signaling through the AhR-integrin signaling axis is mediated primarily through TGF-β_2 (Fig. 6D, top). AhR protein levels were reduced in LN-308 AhRsi cells compared to control cells and altered by integrin inhibition in control, but not in AhRsi cells. Moreover, LN-308 AhRsi cells showed reduced constitutive pSmad2 levels whereas cilengitide inhibition reduced pSmad2 levels more prominently in LN-308 control than in AhRsi cells. As described previously (11), reductions in pSmad2 levels were paralleled by increases in total Smad2 levels, possibly representing a negative feedback loop (Fig. 6D, bottom).

Finally, to confirm the relevance of the identified signaling axis *in vivo*, we performed correlation analyses using data from glioblastoma patients within The Cancer Genome Atlas (TCGA) database. There was a significant correlation of αv integrin and AhR expression (Fig. 7A). For testing these findings on the protein level, we analyzed the levels of integrin αv, AhR and pSmad2 by immunohistochemistry on a tissue microarray of glioblastomas. Again, αv integrin levels correlated with AhR levels. Moreover, a significant correlation of αv integrin with pSmad2 protein levels was observed (Fig. 7B).

Discussion

AhR may act as a tumor promoter by driving several malignant features such as proliferation, clonogenicity and invasiveness in human glioblastoma (8). Antagonism of AhR interferes with TGF-β pathway activity at the level of ligand expression. TGF-β is a multipotent cytokine that has a profound impact on the aggressive phenotype of glioblastoma (19). The TGF-β pathway, in turn, is controlled by the activity of αv integrins in glioma cells (11). AhR has been described as a regulator of the composition of integrins at the cell surface (13, 20-23), but inhibitory effects of AhR on FAK phosphorylation, a central mediator of integrin signaling, have also been observed (14, 24). These findings provided the rationale for the present study, which aimed at elucidating a possible link between the AhR and integrin signaling pathways in modulating the activity of the TGF-β pathway in glioblastoma.

Exposure to αv, β3 or β5 neutralizing antibodies, RNA interference-mediated integrin gene silencing or pharmacological integrin inhibition decreased DRE reporter activity and reduced expression of the AhR target gene CYP1A1 in human long-term as well as glioma-initiating cell lines (Fig. 1, Fig. 2). Integrin inhibition induces detachment of some human glioma cells (16) and AhR activity is induced by suspension in keratinocytes or hepatocytes (25, 26). Moreover, AhR localization may be regulated depending on the density of murine fibroblasts or human keratinocytes. Here, sparse density favored nuclear AhR localization whereas AhR was found predominantly in the cytoplasm at confluence (27, 28). We noticed a reduction in AhR signaling upon integrin inhibition that was not restricted to the adherent cell fraction, but was observed in the floating cell fraction to a similar extent (Fig. 1E). In addition, similar effects were observed in LN-229 or Ha-Cat cells (Fig. 1F, 5C) in which integrin inhibition does not induce detachment or cell death nor affects proliferation (data not shown). These data demonstrate that the observed alterations in AhR signaling upon integrin inhibition are independent from detachment or cellular density.

Investigations regarding the mechanism revealed that reduced AhR reporter activity upon integrin inhibition is not mediated at the transcriptional level, but results from a reduction of AhR total protein levels accompanied by diminished AhR nuclear localization (Fig. 3). In line with these findings, a tight control of the AhR pathway at various levels has been described before. Beside the regulation of AhR at the transcriptional level which is partially controlled by the drug-metabolizing CYP enzymes through an autoregulatory feedback loop, AhR activity is controlled at the level of nucleo-cytoplasmatic shuttling and dissociation from the molecular chaperones, displacement from ARNT by AhR repressor (AhRR), or proteosomal protein degradation (3, 4, 29, 30).

Since antagonism of AhR and integrin inhibition both reduce TGF-β signaling (8, 11), and since integrin inhibition interferes with AhR signaling, we asked whether integrin inhibition-mediated effects on TGF-β signaling are mediated through AhR. Based on this assumption, integrin inhibition-mediated effects on TGF-β signaling should be blunted in murine AhR-null hepatocytes. Constitutive pSmad2 protein levels were similar in control and AhR-null hepatocytes. Indeed, AhR-null cells were less responsive to integrin inhibition-mediated reductions in Smad2 phosphorylation demonstrating that AhR plays a role in linking integrins and TGF-β signaling. However, the partially remaining effect upon integrin inhibition indicates that other regulating mechanisms beside AhR must be involved in controlling TGF-β signaling as well as integrin inhibition-mediated alteration of the TGF-β pathway (Fig. 4C). The mouse cells used for this analysis detach upon integrin inhibition (data not shown) and detachment may alter AhR and TGF-β signaling (11, 25, 26). Accordingly, we used human keratinocytes which do not detach upon integrin inhibition as a model to address the influence of cellular detachment. Silencing of AhR resulted in dramatically reduced AhR and CYP1A1 mRNA expression and integrin inhibition-induced reductions in AhR signaling were abolished in AhRsi cells (Fig. 5A-C). The reduced responsiveness to integrin inhibition-mediated effects on TGF-β_2 mRNA and pSmad2 protein levels in AhRsi cells confirmed that AhR is a central mediator that links integrins

and TGF-β signaling. In line with these data, the results obtained by investigation of AhR-null astrocytes or LN-308 cells with transiently silenced AhR confirmed the importance of this signaling pathway in cells of glial origin, too (Fig. 6). While several studies identified AhR as a transcriptional target of the TGF-β pathway (31, 32), we have shown that in our model integrin inhibitors regulate AhR at a posttranscriptional level. This is due to the observation that AhR mRNA expression was not affected by integrin inhibition while at the same time AhR protein and AhR downstream signaling were reduced, paralleled by a reduction in TGF-β signaling (Fig. 5). Previous publications have reported conflicting findings on the role of AhR for TGF-β expression. Reduced but also elevated TGF-β levels upon activation of the AhR pathway have been observed in a cell type-specific manner (8, 33-36). Our results suggest that AhR may primarily act as a positive regulator of TGF-β signaling, at least in the context of integrin activity. This assumption is further corroborated by a striking correlation of αv integrin expression with nuclear AhR levels and pSmad2 expression in human glioblastomas *in vivo* (Fig. 7). The importance of αv integrin, AhR and pSmad2 expression for the biology of gliomas has been shown before, as their expression correlates with the WHO grade (8, 11, 19). Our data now suggest a close interplay between αv integrin, AhR and pSmad2 expression which may cooperate on a functional level and contribute to the malignant phenotype of glioblastoma. Previous efforts to exploit these targets therapeutically in glioblastoma have been disappointing including a phase III trial on the pentapeptide integrin antagonist cilengitide. In addition, the TGF-β receptor antagonist LY2157299 administered alone or in combination with chemotherapy may not offer a breakthrough in glioblastoma therapy (37, 38). Yet, cilengitide may not have had an optimal pharmacodynamic and pharmacokinetic profile, and LY2157299 may not have been tolerated at doses required to efficiently abrogate TGF-β signaling *in vivo*. The present findings support the ongoing search for more potent integrin inhibitors as well as drugs which interfere with the TGF-β pathway. In summary, we have identified a novel mechanism in which integrin inhibitors

interfere with AhR signaling at a posttranscriptional level, ultimately resulting in reduced TGF-β signaling. These findings validate integrin inhibition as a promising strategy to block both AhR- and TGF-β-controlled features of malignancy in glioblastoma.

Materials and methods

Cells and reagents

The human long-term cell glioma cell lines (LTC) LN-229 and LN-308 were kindly provided by Dr. N. de Tribolet (Lausanne, Switzerland), were recently authenticated by STR profiling and tested for mycoplasma contamination. The generation of LN-229 cells overexpressing constitutive active AhR (CA-AhR) has been described (8). The glioma initiating cells (GIC) ZH-161 and S-24 were established from freshly resected tumors, used during the first passages (39) and cultured in phenol red-free Neurobasal Medium with B-27 supplement (20 µl/ml), Glutamax (10 µl/ml) (Invitrogen, Basel, Switzerland), fibroblast growth factor (FGF)-2, epidermal growth factor (EGF) (20 ng/ml each; Peprotech, Rocky Hill, PA) and heparin (32 IE/ml; Ratiopharm, Ulm, Germany). Hepatocytes, isolated from wildtype or AhR-null neonatal C57BL/6N mice and immortalized with Simian virus 40, were kindly provided by G. H. Perdew (17) and were grown in GIBCO minimum essential medium alpha (Invitrogen), supplemented with 10% fetal calf serum (FCS; Gibco Life Technologies, Paisley, UK), 100 U/ml penicillin and 100 µg/ml streptomycin (Sigma-Aldrich, St. Louis, MO). Doxycycline-inducible AhR knockdown (HaCaT 4.2) or scramble shRNA control cells were generated by lentivirus-mediated transfection (40). The knockdown was induced using 2 µg/ml doxycycline (Sigma-Aldrich). AhR-deficient mice (B6.129-AHR^{tm1Bra}/J) (7), kindly provided by C. Esser (Düsseldorf, Germany), were crossed on a B6.Cg-Tyr^{c-2J}/J background (41) (B6.Cg-Ahr^{tm1Bra} Tyr^{c-2J}) and astrocytes were isolated from AhR$^{-/-}$ or AhR$^{+/-}$ P1 or P2 neonatal mice by seeding the cortical cells for mixed glial cultures on poly-L-lysine (2 µg/cm^2, Sigma-Aldrich)-coated flasks, after cerebral cortices were dissected, freed from the meninges and digested with 0.25 % trypsin and 0.1 mg/ml DNase I (Sigma-Aldrich) for 20 min at 37 °C. At confluence (d7-d9), cultures were treated with 10 µM cytosine arabinoside (Ara-C, Sigma-Aldrich) for 5 days. At the end of Ara-C treatment, cultures were less than 2.5 % CD11b$^+$ as assessed by flow cytometry (data not shown). For *in vitro* experiments, the obtained AhR-null

astrocytes from homozygous ($AhR^{-/-}$) mice or control astrocytes from heterozygous ($AhR^{+/}$) B6.Cg-Ahr^{tm1Bra} Tyr^{c-2J} mice, were grown on poly-L-lysine (2 µg/cm^2)-coated flasks in Dulbecco's Modified Eagle Medium (DMEM; Invitrogen), containing 2 mM L-glutamine (Gibco Life Technologies), 100 U/ml penicillin and 100 µg/ml streptomycin, and 10% FCS. Human LTC were maintained in DMEM, containing 2 mM L-glutamine (Gibco Life Technologies) and 10% FCS, whereas the experiments were carried out in phenol red-free medium without serum, after attachment of the cells. Accutase was purchased from Gibco Life Technologies. Cilengitide (EMD 121974) was kindly supplied by Merck KGaA (Darmstadt, Germany), GLPG0187 by Galapagos NV (Mechelen, Belgium) and the RAD peptide cyclo-(Arg-Ala-Asp-DPhe-Val) was obtained from Bachem AG (Bubendorf, Switzerland). CH-223191 was purchased from Merck, and 3-methylcholanthrene (3-MC) and doxycycline from Sigma Aldrich. The following antibodies were used: phospho-Smad2 (Ser465/467) (clone 138D4) and Smad2 (clone 86F7) were from Cell Signaling Technology (Boston, MA), mouse anti-Smad2/3 antibody was from BD Biosciences, goat polyclonal antibody to actin from Santa Cruz Biotechnology (Santa Cruz, CA) and the mouse monoclonal antibodies to AhR (clone RPT1 for immunoblotting and clone RPT9 for immunofluorescence) were from Abcam (Cambridge, UK). The antibodies to αv (clone 17E6), αvβ3 (clone LM609, MAB1976) and αvβ5 (clone P1F6, MAB1961) were obtained from Merck. The siRNA pool targeting AhR or single integrins and the non-targeting control pool were purchased from Thermo Scientific Dharmacon (Lafayette, CO) and used at 100 nM. Transient lipophilic transfection was performed with Metafectene Pro (Biontex, Martinsried, Germany).

Real-time PCR

Total RNA was isolated using the NucleoSpin RNA II system from Macherey-Nagel (Düren, Germany) and cDNA was prepared using the High Capacity cDNA Reverse Transcription Kit from Applied Biosystems (Foster City, CA). Gene expression was measured in an ABI Prism 7000 Sequence Detection System (Applied Biosystems) using SYBR Green Master Mix from

Thermo Fisher Scientific (Waltham, MA) and primers from Microsynth AG (Balgach, Switzerland) at optimized concentrations. Glyceraldehyde 3-phosphate dehydrogenase primers have been described (42). Primer sequences were as follows: human AhR, forward 5′-GGCTCAGGTTATCAGTTTATT (NM_001621.3, nt 1537–1557), reverse 5′-ACTATCATGCCACTTTCTCC-3′ (NM_001621.3, nt 1612–1631), human CYP1A1, forward 5′-CAGCTGGATGAGAACGCCAAT-3′ (NM_000499.3, nt 999–1019), reverse 5′-GTGTCAAACCCAGCTCCAAAG (NM_000499.3, nt 1064–1083)), human TGF-β_1, forward 5′-GCCCTGGACACCAACTATTG-3′ (NM_000660.3, nt 1702–1727), reverse 5′-CGTGTCCAGGCTCCAAATG-3′ (NM_000660.3, nt 1851–1869), human TGF-β_2, forward 5′-AAGCTTACACTGTCCCTGCTGC-3′ (NM_003238.1, nt 847–868), reverse 5′-TGTGGAGGTGCCATCAATACCT-3′ (NM_003228.1, nt 934–955), mouse HPRT1, forward 5′-TTGCTGACCTGCTGGATTAC-3′ (NM_013556.2, nt 370-389), reverse 5′-TTTATGTCCCCCGTTGACTG-3′ (NM_013556.2, nt 471-490), mouse AhR, forward 5′-AGCCGGTGCAGAAAACAGTAA-3′ (NM_01346, nt 47-67), reverse 5′-AGGCGGTCTAACTCTGTGTTC-3′ (NM_01346, nt 126-146), mouse CYP1A1, forward 5′-CAATGAGTTTGGGGAGGTTACTG-3′ (NM_009992, 675-697), reverse 5′-CCCTTCTCAAATGTCCTGTAGTG-3′ (NM_009992, 817-839), mouse TGF-β_1, forward 5′-CTCCCGTGGCTTCTAGTGC-3′ (NM_011577.1, 910-928), reverse 5′-GCCTTAGTTTGGACAGGATCTG-3′ (NM_011577.1, 1021-1042) and mouse TGF-β_2, forward 5′-TCGACATGGATCAGTTTATGCG-3′ (NM_009367.3, 1298-1319), reverse 5′-CCCTGGTACTGTTGTAGATGGA-3′ (NM_009367.3, 1423-1444). The conditions were 40 cycles at 95°C/15 s and 60°C/1 min. Standard curves were generated for each gene. Relative quantification of gene expression was determined by comparison of threshold values. All results were normalized to the house keeping gene and calculated with the ΔCTT method for relative quantification (39).

Immunoblot analysis

Whole cell lysates were prepared by lysing cells in radioimmunoprecipitation assay (RIPA) buffer (10 mM Tris pH 8.0, 150 mM NaCl, 1% NP-40, 0.5% deoxycholate, 0.1% sodium dodecyl sulfate) supplemented with 1x complete inhibitor mix (Roche Diagnostics, Grenzach-Wyhlen, Germany) and phosphatase inhibitor cocktails 1 and 2 (Sigma-Aldrich). Fractionated lysates were prepared using the NE-PER Nuclear and Cytoplasmic Extraction Kit from Thermo Fisher Scientific. Protein levels were analyzed by immunoblot using 30 µg of protein per lane mixed with Laemmli buffer containing β-mercaptoethanol and by visualizing protein bands with horseradish peroxidase (HRP)-coupled secondary antibodies (Sigma-Aldrich) and enhanced chemiluminescence (Perbio, Bonn, Germany). Quantification of the density of protein bands was done with ImageJ software (U. S. National Institutes of Health, Bethesda, MD).

Flow cytometry

For detection of AhR intracellular protein levels, cells were detached with accutase and permeabilized using the Fix/Perm Buffer Set (Biolegend, San Diego, CA) followed by incubation with anti-human AhR-PE antibody (eBioscience, San Diego, CA) or isotype control, diluted in PBS containing 0.5% bovine serum albumin, 2 mM EDTA and 1 mM $MgCl_2$. Intracellular expression levels were determined using a CyAn flow cytometer (Beckman Coulter, Nyon, Switzerland).

Immunofluorescence

Immunofluorescence studies were carried out on cytospins (5 x 10^5 cells/slide). Samples were dried for 30 min and fixed in ice-cold methanol:aceton (1:1). AhR staining was performed as described (8) and binding specificity was controlled by IgG isotype control (Jackson Immunoresearch, Suffolk, UK).

Gene reporter assay

Dual luciferase/renilla assays were performed with co-transfection of 150 ng of the pT81/3 x DRE reporter construct, containing the DRE3 from the CYP enhancer region (43), and 20 ng of renilla reniformis-CMV (pRL-CMV) control plasmid (Promega, WI). LN-229 cells were transfected with 75 ng of the pT81/3 x DRE reporter construct, 75 ng of the co-plasmid pARNT (44) and 20 ng of pRL-CMV. Luciferase activity was normalized to constitutive renilla activity.

TCGA analysis

Analysis within the TCGA database (http://cancergenome.nih.gov) was done for the glioblastoma 540 - MAS5.0 - u133a dataset (n=540) using the module for correlation of 2 genes of the R2: microarray analysis and visualization platform (http://r2.amc.nl).

Immunohistochemistry

Glioblastomas were analyzed on a tissue microarray (TMA). The TMA, kindly provided by Karl Frei (Department of Neurosurgery, Zurich), contained tissue of 47 glioblastomas as previously described (45). TMA sections were stained using the rabbit monoclonal primary antibody anti-integrin pan-αv (clone EM01309, 1:10.000), the rabbit polyclonal antibody anti-pSmad2 (clone 138D4, 1:200) and the mouse monoclonal antibody anti-AhR (clone BHLHE76, 1:200) (8, 46, 47). The intensity of staining and the percentage of stained tumor cells were calculated as the percentage of weakly stained cells plus the percentage of moderately stained cells multiplied by two plus the percentage of strongly stained cells multiplied by three and results were expressed as H scores ranging from 0 – 300 (48, 49). A Pearson correlation test was performed using Prism 5 (GraphPad Software, San Diego, CA).

Statistical analysis

Data are presented as means and SEM for real-time PCR experiments and as means and SD for all the other experiments. The experiments shown were repeated at least two to three times. Gene reporter assays were performed using at least triplicate wells, whereas real-time PCR was performed at least in duplicates. Analysis of significance was performed using a two-tailed Student's t-test (Excel, Microsoft, Redmond, WA) (*$p<0.05$, **$p<0.01$).

Conflict of interest:

PR has received honoraria for lectures or advisory board participation from MSD, Roche, Novartis and Molecular Partners. MW has received research grants from Acceleron, Actelion, Alpinia Institute, Bayer, Isarna, MSD, Merck & Co, Novocure, PIQUR and Roche and honoraria for lectures or advisory board participation or consulting from Celldex, Immunocellular, Isarna, Magforce, MSD, Merck & Co, Northwest Biotherapeutics, Novocure, Pfizer, Roche and Teva. MP has received research grants from Bayer, Merck, Novartis and Nuon Biotherapeutics and honoraria for lectures or advisory board participation or consulting from Bayer, Merck, Novartis, Roche, Alexion, MSD, iTEOS and Miltenyi. All other authors declare no conflicts of interest.

Acknowledgements:

This study was supported by grants from the Novartis Foundation for medical-biological research and the Kurt und Senta Herrmann Foundation to PR and the Heidelberg University Innovation Fund FRONTIER to MP.

References

1. Denison MS, Rogers JM, Rushing SR, Jones CL, Tetangco SC, Heath-Pagliuso S. Analysis of the aryl hydrocarbon receptor (AhR) signal transduction pathway. Curr Protoc Toxicol. 2002;Chapter 4:Unit4 8.

2. Nguyen LP, Bradfield CA. The search for endogenous activators of the aryl hydrocarbon receptor. Chem Res Toxicol. 2008;21(1):102-16.

3. Stockinger B, Di Meglio P, Gialitakis M, Duarte JH. The aryl hydrocarbon receptor: multitasking in the immune system. Annu Rev Immunol. 2014;32:403-32.

4. Dietrich C, Kaina B. The aryl hydrocarbon receptor (AhR) in the regulation of cell-cell contact and tumor growth. Carcinogenesis. 2010;31(8):1319-28.

5. Feng S, Cao Z, Wang X. Role of aryl hydrocarbon receptor in cancer. Biochim Biophys Acta. 2013;1836(2):197-210.

6. Safe S, Lee SO, Jin UH. Role of the aryl hydrocarbon receptor in carcinogenesis and potential as a drug target. Toxicol Sci. 2013;135(1):1-16.

7. Opitz CA, Litzenburger UM, Sahm F, Ott M, Tritschler I, Trump S, et al. An endogenous tumour-promoting ligand of the human aryl hydrocarbon receptor. Nature. 2011;478(7368):197-203.

8. Gramatzki D, Pantazis G, Schittenhelm J, Tabatabai G, Kohle C, Wick W, et al. Aryl hydrocarbon receptor inhibition downregulates the TGF-beta/Smad pathway in human glioblastoma cells. Oncogene. 2009;28(28):2593-605.

9. Joseph JV, Balasubramaniyan V, Walenkamp A, Kruyt FA. TGF-beta as a therapeutic target in high grade gliomas - promises and challenges. Biochem Pharmacol. 2013;85(4):478-85.

10. Seoane J, Le HV, Shen L, Anderson SA, Massague J. Integration of Smad and forkhead pathways in the control of neuroepithelial and glioblastoma cell proliferation. Cell. 2004;117(2):211-23.

11. Roth P, Silginer M, Goodman SL, Hasenbach K, Thies S, Maurer G, et al. Integrin control of the transforming growth factor-beta pathway in glioblastoma. Brain. 2013;136(Pt 2):564-76.

12. Desgrosellier JS, Cheresh DA. Integrins in cancer: biological implications and therapeutic opportunities. Nat Rev Cancer. 2010;10(1):9-22.

13. Kung T, Murphy KA, White LA. The aryl hydrocarbon receptor (AhR) pathway as a regulatory pathway for cell adhesion and matrix metabolism. Biochem Pharmacol. 2009;77(4):536-46.

14. Juan SH, Lee JL, Ho PY, Lee YH, Lee WS. Antiproliferative and antiangiogenic effects of 3-methylcholanthrene, an aryl-hydrocarbon receptor agonist, in human umbilical vascular endothelial cells. Eur J Pharmacol. 2006;530(1-2):1-8.

15. Nebert DW, Dalton TP, Okey AB, Gonzalez FJ. Role of aryl hydrocarbon receptor-mediated induction of the CYP1 enzymes in environmental toxicity and cancer. J Biol Chem. 2004;279(23):23847-50.

16. Maurer GD, Tritschler I, Adams B, Tabatabai G, Wick W, Stupp R, et al. Cilengitide modulates attachment and viability of human glioma cells, but not sensitivity to irradiation or temozolomide in vitro. Neuro Oncol. 2009;11(6):747-56.

17. Murray IA, Reen RK, Leathery N, Ramadoss P, Bonati L, Gonzalez FJ, et al. Evidence that ligand binding is a key determinant of Ah receptor-mediated transcriptional activity. Arch Biochem Biophys. 2005;442(1):59-71.

18. Silginer M, Weller M, Ziegler U, Roth P. Integrin inhibition promotes atypical anoikis in glioma cells. Cell Death Dis. 2014;5:e1012.

19. Bruna A, Darken RS, Rojo F, Ocana A, Penuelas S, Arias A, et al. High TGFbeta-Smad activity confers poor prognosis in glioma patients and promotes cell proliferation depending on the methylation of the PDGF-B gene. Cancer Cell. 2007;11(2):147-60.

20. Prell RA, Kerkvliet NI. Involvement of altered B7 expression in dioxin immunotoxicity: B7 transfection restores the CTL but not the autoantibody response to the P815 mastocytoma. J Immunol. 1997;158(6):2695-703.

21. Riecke K, Schmidt A, Stahlmann R. Effects of 2,3,7,8-TCDD and PCB 126 on human thymic epithelial cells in vitro. Arch Toxicol. 2003;77(6):358-64.

22. Monteiro P, Gilot D, Le Ferrec E, Lecureur V, N'Diaye M, Le Vee M, et al. AhR- and c-maf-dependent induction of beta7-integrin expression in human macrophages in response to environmental polycyclic aromatic hydrocarbons. Biochem Biophys Res Commun. 2007;358(2):442-8.

23. Abe Y, Sinozaki H, Takagi T, Minegishi T, Kokame K, Kangawa K, et al. Identification of 2,3,7,8-tetrachlorodibenzo-p-dioxin (TCDD)-inducible genes in human amniotic epithelial cells. Reprod Biol Endocrinol. 2006;4:27.

24. Mulero-Navarro S, Pozo-Guisado E, Perez-Mancera PA, Alvarez-Barrientos A, Catalina-Fernandez I, Hernandez-Nieto E, et al. Immortalized mouse mammary fibroblasts lacking dioxin receptor have impaired tumorigenicity in a subcutaneous mouse xenograft model. J Biol Chem. 2005;280(31):28731-41.

25. Sadek CM, Allen-Hoffmann BL. Suspension-mediated induction of Hepa 1c1c7 Cyp1a-1 expression is dependent on the Ah receptor signal transduction pathway. J Biol Chem. 1994;269(50):31505-9.

26. Sadek CM, Allen-Hoffmann BL. Cytochrome P450IA1 is rapidly induced in normal human keratinocytes in the absence of xenobiotics. J Biol Chem. 1994;269(23):16067-74.

27. Ikuta T, Kobayashi Y, Kawajiri K. Cell density regulates intracellular localization of aryl hydrocarbon receptor. J Biol Chem. 2004;279(18):19209-16.

28. Cho YC, Zheng W, Jefcoate CR. Disruption of cell-cell contact maximally but transiently activates AhR-mediated transcription in 10T1/2 fibroblasts. Toxicol Appl Pharmacol. 2004;199(3):220-38.

29. Mimura J, Ema M, Sogawa K, Fujii-Kuriyama Y. Identification of a novel mechanism of regulation of Ah (dioxin) receptor function. Genes Dev. 1999;13(1):20-5.

30. Davarinos NA, Pollenz RS. Aryl hydrocarbon receptor imported into the nucleus following ligand binding is rapidly degraded via the cytosplasmic proteasome following nuclear export. J Biol Chem. 1999;274(40):28708-15.

31. Dohr O, Sinning R, Vogel C, Munzel P, Abel J. Effect of transforming growth factor-beta1 on expression of aryl hydrocarbon receptor and genes of Ah gene battery: clues for independent down-regulation in A549 cells. Mol Pharmacol. 1997;51(5):703-10.

32. Wolff S, Harper PA, Wong JM, Mostert V, Wang Y, Abel J. Cell-specific regulation of human aryl hydrocarbon receptor expression by transforming growth factor-beta(1). Mol Pharmacol. 2001;59(4):716-24.

33. Gaido KW, Maness SC, Leonard LS, Greenlee WF. 2,3,7,8-Tetrachlorodibenzo-p-dioxin-dependent regulation of transforming growth factors-alpha and -beta 2 expression in a human keratinocyte cell line involves both transcriptional and post-transcriptional control. J Biol Chem. 1992;267(34):24591-5.

34. Vogel C, Abel J. Effect of 2,3,7,8-tetrachlorodibenzo-p-dioxin on growth factor expression in the human breast cancer cell line MCF-7. Arch Toxicol. 1995;69(4):259-65.

35. Corchero J, Martin-Partido G, Dallas SL, Fernandez-Salguero PM. Liver portal fibrosis in dioxin receptor-null mice that overexpress the latent transforming growth factor-beta-binding protein-1. Int J Exp Pathol. 2004;85(5):295-302.

36. Santiago-Josefat B, Mulero-Navarro S, Dallas SL, Fernandez-Salguero PM. Overexpression of latent transforming growth factor-beta binding protein 1 (LTBP-1) in dioxin receptor-null mouse embryo fibroblasts. J Cell Sci. 2004;117(Pt 6):849-59.

37. Stupp R, Hegi ME, Gorlia T, Erridge SC, Perry J, Hong YK, et al. Cilengitide combined with standard treatment for patients with newly diagnosed glioblastoma with methylated MGMT promoter (CENTRIC EORTC 26071-22072 study): a multicentre, randomised, open-label, phase 3 trial. Lancet Oncol. 2014;15(10):1100-8.

38. Rodon J, Carducci M, Sepulveda-Sanchez JM, Azaro A, Calvo E, Seoane J, et al. Pharmacokinetic, pharmacodynamic and biomarker evaluation of transforming growth factor-beta receptor I kinase inhibitor, galunisertib, in phase 1 study in patients with advanced cancer. Invest New Drugs. 2014.

39. Codo P, Weller M, Meister G, Szabo E, Steinle A, Wolter M, et al. MicroRNA-mediated down-regulation of NKG2D ligands contributes to glioma immune escape. Oncotarget. 2014;5(17):7651-62.

40. Hao N, Lee KL, Furness SG, Bosdotter C, Poellinger L, Whitelaw ML. Xenobiotics and loss of cell adhesion drive distinct transcriptional outcomes by aryl hydrocarbon receptor signaling. Mol Pharmacol. 2012;82(6):1082-93.

41. Townsend D, Witkop CJ, Jr., Mattson J. Tyrosinase subcellular distribution and kinetic parameters in wild type and C-locus mutant C57BL/6J mice. J Exp Zool. 1981;216(1):113-9.

42. Carraro G, Albertin G, Forneris M, Nussdorfer GG. Similar sequence-free amplification of human glyceraldehyde-3-phosphate dehydrogenase for real time RT-PCR applications. Mol Cell Probes. 2005;19(3):181-6.

43. Kress S, Reichert J, Schwarz M. Functional analysis of the human cytochrome P4501A1 (CYP1A1) gene enhancer. Eur J Biochem. 1998;258(2):803-12.

44. Mason GG, Witte AM, Whitelaw ML, Antonsson C, McGuire J, Wilhelmsson A, et al. Purification of the DNA binding form of dioxin receptor. Role of the Arnt cofactor in regulation of dioxin receptor function. J Biol Chem. 1994;269(6):4438-49.

45. Wirsching HG, Krishnan S, Florea AM, Frei K, Krayenbuhl N, Hasenbach K, et al. Thymosin beta 4 gene silencing decreases stemness and invasiveness in glioblastoma. Brain. 2014;137(Pt 2):433-48.

46. Goodman SL, Grote HJ, Wilm C. Matched rabbit monoclonal antibodies against alphav-series integrins reveal a novel alphavbeta3-LIBS epitope, and permit routine staining of archival paraffin samples of human tumors. Biol Open. 2012;1(4):329-40.

47. Frei K, Gramatzki D, Tritschler I, Schroeder JJ, Espinoza L, Rushing EJ, et al. Transforming growth factor-beta pathway activity in glioblastoma. Oncotarget. 2015;6(8):5963-77.

48. Kraus JA, Dabbs DJ, Beriwal S, Bhargava R. Semi-quantitative immunohistochemical assay versus oncotype DX((R)) qRT-PCR assay for estrogen and progesterone receptors: an independent quality assurance study. Mod Pathol. 2012;25(6):869-76.

49. Kinsel LB, Szabo E, Greene GL, Konrath J, Leight GS, McCarty KS, Jr. Immunocytochemical analysis of estrogen receptors as a predictor of prognosis in breast cancer patients: comparison with quantitative biochemical methods. Cancer Res. 1989;49(4):1052-6.

Figure legends

Fig. 1. Integrin inhibition mediates suppression of AhR activity in human glioma cells. A, B. LN-308 cells were exposed to RAD (10 µM) or cilengitide (1, 10 or 100 µM) (A), DMSO control or GLPG0187 (0.0001, 0.01 or 1 µM) (B) or CH-223191 (10 µM, AhR antagonist) for 24 h. AhR activity was determined by reporter assays (* $p < 0.05$; ** $p < 0.01$, relative to cells exposed to RAD (A) or DMSO (B)). C. LN-308 glioma cells were co-cultured with neutralizing antibodies at 10 µg/ml to different integrins as indicated or CH-223191 (10 µM). DRE reporter activity was analyzed after 24 h (** $p < 0.01$, relative to cells exposed to isotype control). D. LN-308 cells were transiently transfected with siRNA oligonucleotides specific for one integrin or a control siRNA. AhR activity was determined by reporter assay (* $p < 0.05$; ** $p < 0.01$, relative to cells transfected with control siRNA). E. LN-308 cells were exposed to RAD, cilengitide (1 µM or 10 µM), CH-223191 (10 µM) or 3-methylcholanthrene (1.5 µM, 3-MC, AhR agonist) for 6 h. Floating and adherent cell fractions were harvested separately F. LN-229 cells were exposed to RAD, cilengitide (0.1, 1 or 10 µM), CH-223191 (10 µM) or 3-MC (1.5 µM) for 24 h (right). AhR activity was determined by reporter assay (** $p < 0.01$, relative to cells exposed to RAD). G-J. LN-308 cells were exposed to RAD, cilengitide (10 µM), CH-223191 (10 µM) or 3-MC (1.5 µM) for 48 h (G) or to DMSO control or GLPG0187 (1 µM) for 12, 24 or 48 h (H). The cells were exposed to integrin neutralizing antibodies for 48 h (I) or treated with the indicated integrin siRNA oligonucleotides for 48 h (J). CYP1A1 mRNA expression levels were determined by real-time PCR and normalized to GAPDH.

Fig. 2. Integrin inhibition reduces AhR activity in human GIC. A. ZH-161 or S-24 GIC were exposed to RAD, cilengitide (1 or 10 µM) or CH-223191 (10 µM) for 24 h and analyzed for AhR activity using reporter assays (* $p < 0.05$; ** $p < 0.01$, relative to cells exposed to RAD). B. ZH-161 or S-24 GIC were exposed to DMSO control, GLPG0187 (0.1 or 1 µM) or CH-223191 (10

μM) for 24 h. AhR activity was analyzed by reporter assays (* $p < 0.05$; ** $p < 0.01$, relative to cells exposed to DMSO). C. ZH-161 or S-24 cells were exposed to RAD or cilengitide (10 μM, left), or DMSO or GLPG0187 (10 μM, right) for 72 h. CYP1A1 mRNA expression levels were determined by real-time PCR and normalized to GAPDH (* $p < 0.05$; ** $p < 0.01$, relative to cells exposed to DMSO).

Fig. 3. Integrin inhibition reduces AhR total and nuclear protein levels. A. LN-308 cells were exposed to RAD, cilengitide (10 μM), CH-223191 (10 μM) or 3-MC (1.5 μM) for 48 h (top), to DMSO control or GLPG0187 (1 μM) for the indicated time points (middle) or were transiently transfected with siRNA oligonucleotides specific for one integrin or a control siRNA (bottom). AhR mRNA expression levels were determined by real-time PCR after 48 h. B. LN-229 control or AhR-CA cells were exposed to RAD or cilengitide (0.1, 1 μM or 10 μM) for 24 h and analyzed for AhR activity by reporter assays (bars representing the absolute values, dotted lines representing the values relative to RAD; * $p < 0.05$; ** $p < 0.01$, relative to cells exposed to RAD; $^{+}$ $p < 0.05$; $^{++}$ $p < 0.01$, relative to control transfected cells) (top). LN-229 control or AhR-CA cells were exposed to RAD or cilengitide (10 μM) for 48 h. CYP1A1 mRNA expression levels were assessed by real-time PCR (bottom). C. Whole cell protein lysates of LN-308 cells exposed to control peptide or cilengitide (1 μM or 10 μM) for 24 h were assessed for AhR, pSmad2 or Smad2 protein levels by immunoblot using actin as a loading control. D. Fractionated lysates of LN-308 cells exposed to RAD or cilengitide (10 μM) for 24 h were analyzed for AhR protein levels, using GAPDH as a control for fractionation and actin as a loading control (top). AhR protein levels were normalized to actin (bottom). E. LN-308 cells were exposed to RAD or cilengitide (10 μM) for 24 h. AhR expression levels were analyzed by immunofluorescence (green). Nuclei were stained with DAPI (blue).

Fig. 4: AhR gene silencing abrogates integrin inhibition-mediated effects on TGF-β signaling in murine hepatocytes. A. Murine $AhR^{+/+}$ or $AhR^{-/-}$ hepatocytes were exposed to control peptide or cilengitide (10 µM) for 24 h. AhR (top) and CYP1A1 (bottom) mRNA levels were assessed by real-time PCR. HPRT1 was used as an internal control ($^{+}$ $p < 0.05$; $^{++}$ $p < 0.01$, relative to control cells). B. Murine $AhR^{+/+}$ or $AhR^{-/-}$ hepatocytes were treated with RAD or increasing concentrations of cilengitide as indicated or CH-223191 for 24 h and DRE reporter activity was determined (bars representing the absolute values, dotted lines representing the values relative to RAD; * $p < 0.05$; ** $p < 0.01$, relative to RAD exposure; $^{++}$ $p < 0.01$, relative to control cells). C. Whole cell lysates of $AhR^{+/+}$ or $AhR^{-/-}$ cells exposed to RAD or cilengitide (10 µM) for 4 h were analyzed for pSmad2 and Smad2-3 protein levels. Actin was used as a loading control.

Fig. 5: AhR silencing interferes with the control of the TGF-β pathway by integrin inhibitors in human keratinocytes. A. Human HaCaT control or AhRsi cells were exposed to RAD or cilengitide (10 µM) for 48 h. AhR (top) or CYP1A1 (bottom) mRNA expression levels were assessed by real-time PCR using GAPDH as an internal control (* $p < 0.05$, relative to RAD exposure; $^{+}$ $p < 0.05$; $^{++}$ $p < 0.01$, relative to control cells). B. HaCaT control or AhRsi cells were exposed to RAD or cilengitide (10 µM) for 24 h. AhR expression levels were assessed by flow cytometry upon permeabilization of the cells. C. Human HaCaT control or AhRsi cells were treated with RAD or increasing concentrations of cilengitide as indicated for 24 h and DRE reporter activity was determined (bars representing absolute values, dotted lines representing the values relative to RAD control; ** $p < 0.01$, relative to cells exposed to RAD). D. HaCaT control or AhRsi cells were exposed to RAD or cilengitide (10 µM) for 48 h. TGF-β_1 and TGF-β_2 mRNA expression levels were assessed by real-time PCR using GAPDH as an internal control (** $p < 0.05$, relative to RAD exposure; $^{+}$ $p < 0.05$, relative to control cells). E. Whole cell lysates of HaCaT control or AhRsi cells, exposed to RAD or cilengitide (10 µM) for 48 h, were analyzed

for AhR, pSmad2 or Smad2 protein levels. Actin was used as a loading control (left). pSmad2 protein levels were normalized to actin (right).

Fig. 6: AhR silencing interferes with the control of the TGF-β pathway by integrin inhibitors in cells of glial origin. A. Control or AhR-null astrocytes were exposed to control peptide or cilengitide (10 µM) for 72 h. AhR (top), CYP1A1 (middle) or TGF-β_2 (bottom) mRNA levels were assessed by real-time PCR. HPRT1 was used as an internal control (* $p < 0.05$, relative to RAD exposure; ++ $p < 0.01$, relative to control cells). B. LN-308 cells were transiently transfected with siRNA specific for AhR or control siRNA. After 24 h, the cells were exposed to RAD or cilengitide (10 µM) for 48 h and AhR (top) or CYP1A1 (bottom) mRNA expression levels were assessed by real-time PCR using GAPDH as an internal control (++ $p < 0.01$, relative to control cells). C. Whole cell lysates of LN-308 control or AhRsi cells, exposed to RAD or cilengitide (10 µM) for 24 h, were analyzed for AhR using actin as a loading control (top). Control or AhRsi cells were exposed to RAD, cilengitide (1 or 10 µM) or CH-223131 (10 µM) for 48 h and DRE reporter activity was determined (** $p < 0.01$, relative to cells exposed to RAD; ++ $p < 0.01$, relative to control transfectants) (bottom). D. LN-308 control or AhRsi cells were treated as in (B) and TGF-β_1 and TGF-β_2 mRNA expression levels were assessed by real-time PCR using GAPDH as an internal control (** $p < 0.05$, relative to RAD exposure; ++ $p < 0.05$, relative to control cells) (top). Whole cell lysates of LN-308 control or AhRsi cells, exposed to RAD or cilengitide (10 µM) for 48 h, were analyzed for pSmad2 or Smad2 protein levels, using actin as a loading control (bottom, left). pSmad2 protein levels were normalized to actin (bottom, right).

Fig. 7: αv integrin expression correlates with AhR nuclear levels *in vivo*. A. Correlation analyses of αv integrin with AhR mRNA levels in glioblastoma patients from the TCGA database. Two-tailed Pearson test coefficients (r) and significances (p) are indicated. B. Integrin pan-αv, pSmad2 or nuclear AhR protein levels were assessed by immunohistochemistry on a

glioblastoma tissue microarray (TMA) and correlation analyses were performed. Two-tailed Pearson test coefficients (r) and significances (p) are indicated (top). Representative images of a tumor with low expression profile of αv integrin, AhR and pSmad2 (left) and a tumor with high expression levels of the respective markers (right) are shown and corresponding H scores are indicated (scale bar, 100 µm) (bottom).

Fig. 1

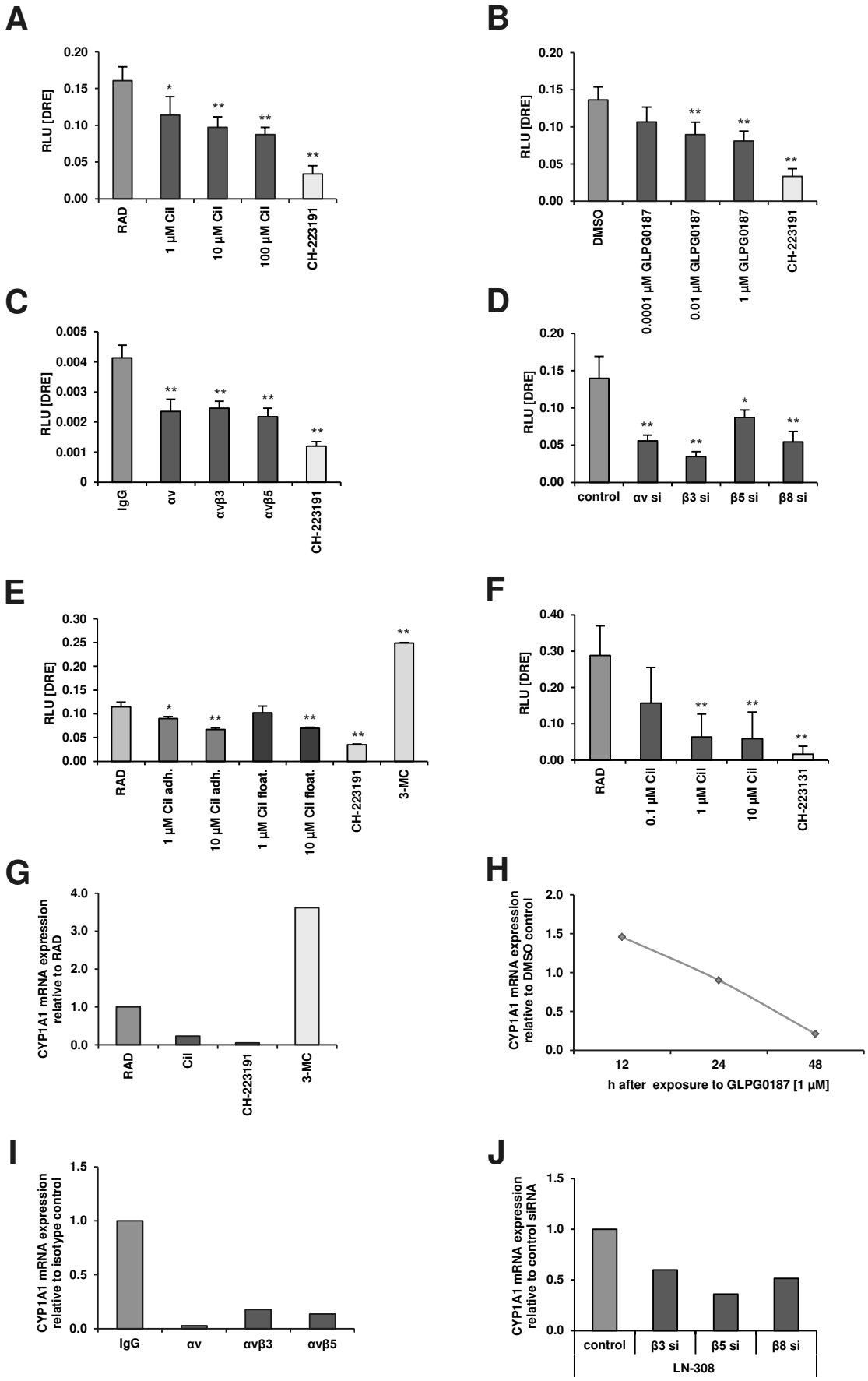
A
RLU [DRE]
0.20
0.15
0.10
0.05
0.00
RAD
1 µM Cil
10 µM Cil
100 µM Cil
CH-223191
B
RLU [DRE]
DMSO
0.0001 µM GLPG0187
0.01 µM GLPG0187
1 µM GLPG0187
CH-223191
C
RLU [DRE]
0.005
0.004
0.003
0.002
0.001
0
IgG
αv
αvβ3
αvβ5
CH-223191
D
RLU [DRE]
control
αv si
β3 si
β5 si
β8 si
E
RLU [DRE]
RAD
1 µM Cil adh.
10 µM Cil adh.
1 µM Cil float.
10 µM Cil float.
CH-223191
3-MC
F
RLU [DRE]
RAD
0.1 µM Cil
1 µM Cil
10 µM Cil
CH-223131
G
CYP1A1 mRNA expression relative to RAD
RAD
Cil
CH-223191
3-MC
H
CYP1A1 mRNA expression relative to DMSO control
12
24
48
h after exposure to GLPG0187 [1 µM]
I
CYP1A1 mRNA expression relative to isotype control
IgG
αv
αvβ3
αvβ5
J
CYP1A1 mRNA expression relative to control siRNA
control
β3 si
β5 si
β8 si
LN-308

Fig. 2

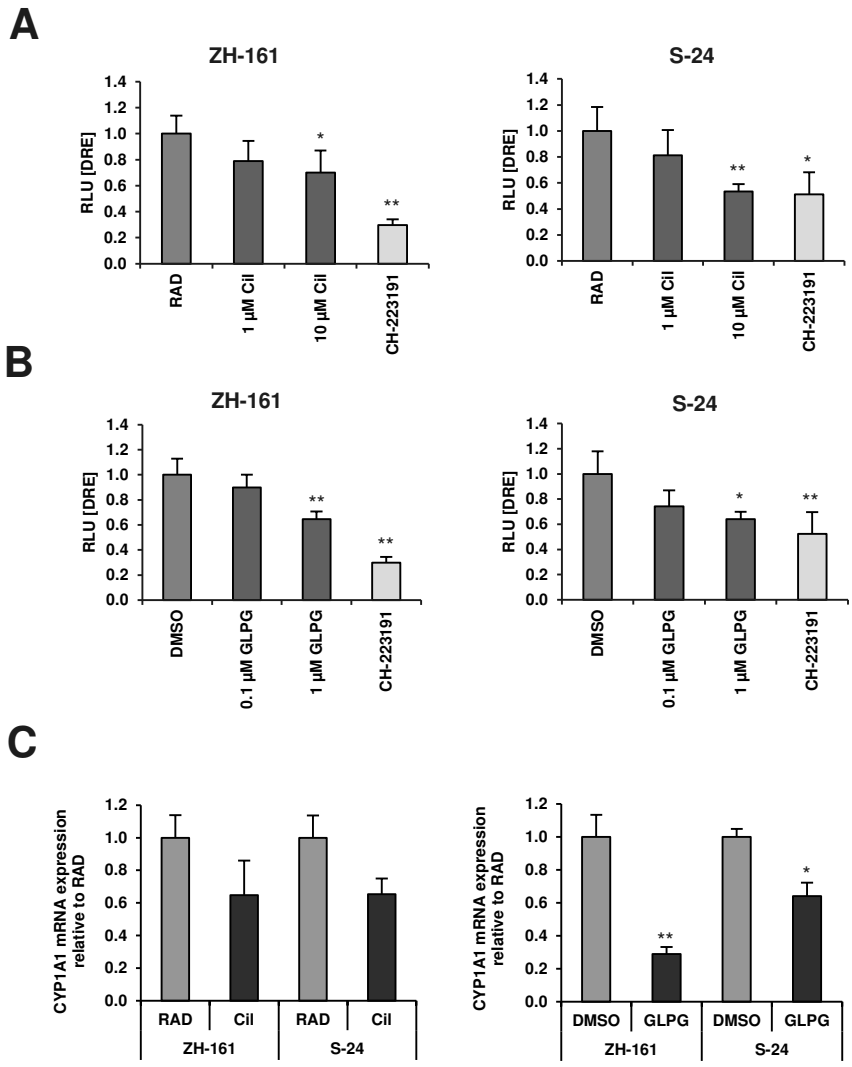
A
ZH-161
S-24
RLU [DRE]
1.4
1.2
1.0
0.8
0.6
0.4
0.2
0.0
*
**
RAD
1 µM CIl
10 µM CIl
CH-223191
B
ZH-161
S-24
RLU [DRE]
**
*
DMSO
0.1 µM GLPG
1 µM GLPG
CH-223191
C
CYP1A1 mRNA expression relative to RAD
1.2
1.0
0.8
0.6
0.4
0.2
0.0
RAD
CIl
ZH-161
S-24
DMSO
GLPG

Fig. 3

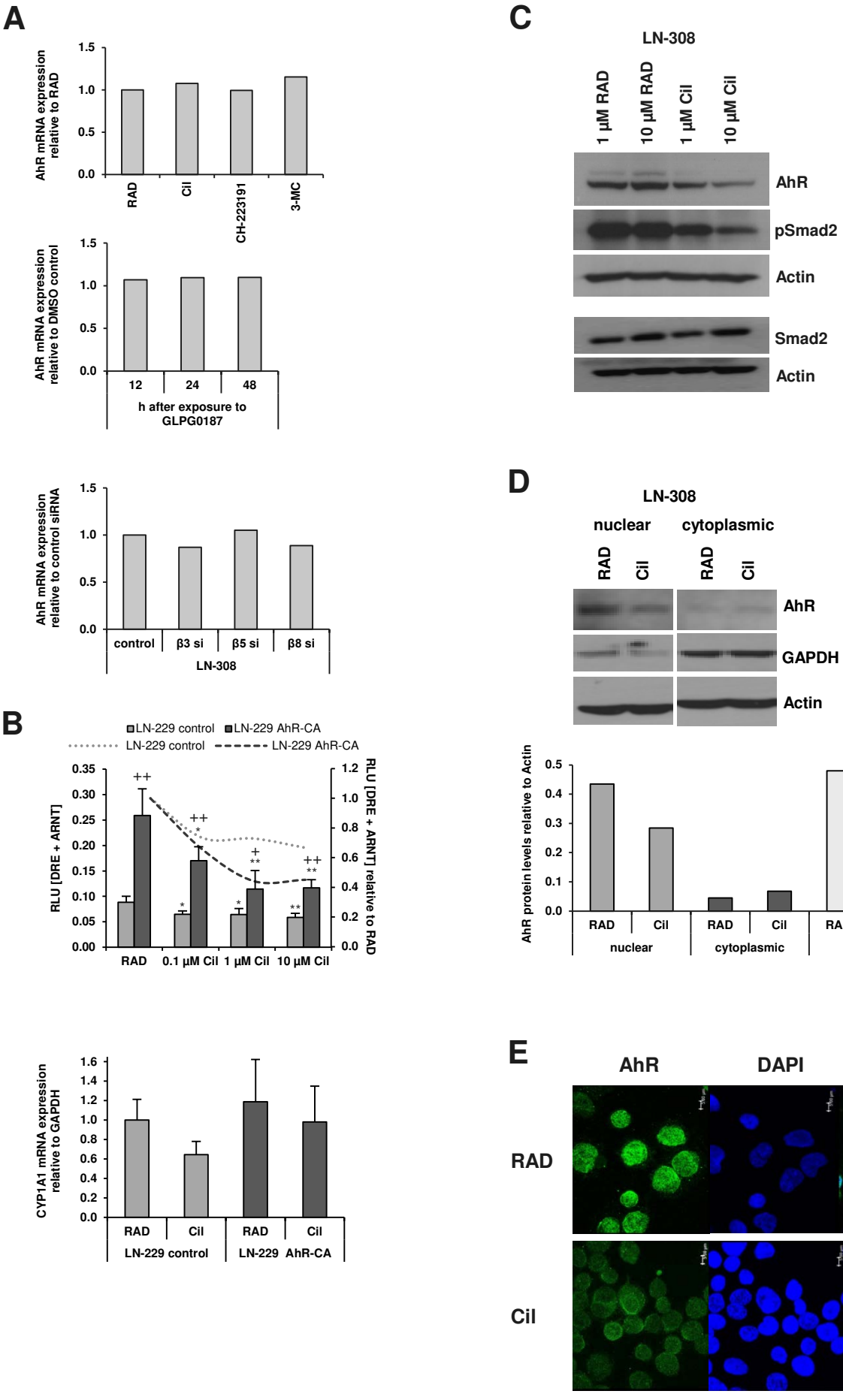
A
AhR mRNA expression relative to RAD
RAD
Cil
CH-223191
3-MC
AhR mRNA expression relative to DMSO control
12
24
48
h after exposure to GLPG0187
AhR mRNA expression relative to control siRNA
control
β3 si
β5 si
β8 si
LN-308
B
LN-229 control
LN-229 AhR-CA
RLU [DRE + ARNT]
RLU [DRE + ARNT] relative to RAD
RAD
0.1 μM Cil
1 μM Cil
10 μM Cil
CYP1A1 mRNA expression relative to GAPDH
LN-229 control
LN-229 AhR-CA
C
LN-308
1 μM RAD
10 μM RAD
1 μM Cil
10 μM Cil
AhR
pSmad2
Actin
Smad2
Actin
D
LN-308
nuclear
cytoplasmic
AhR
GAPDH
Actin
AhR protein levels relative to Actin
nuclear
cytoplasmic
total
E
AhR
DAPI
merge
RAD
Cil

Fig. 4

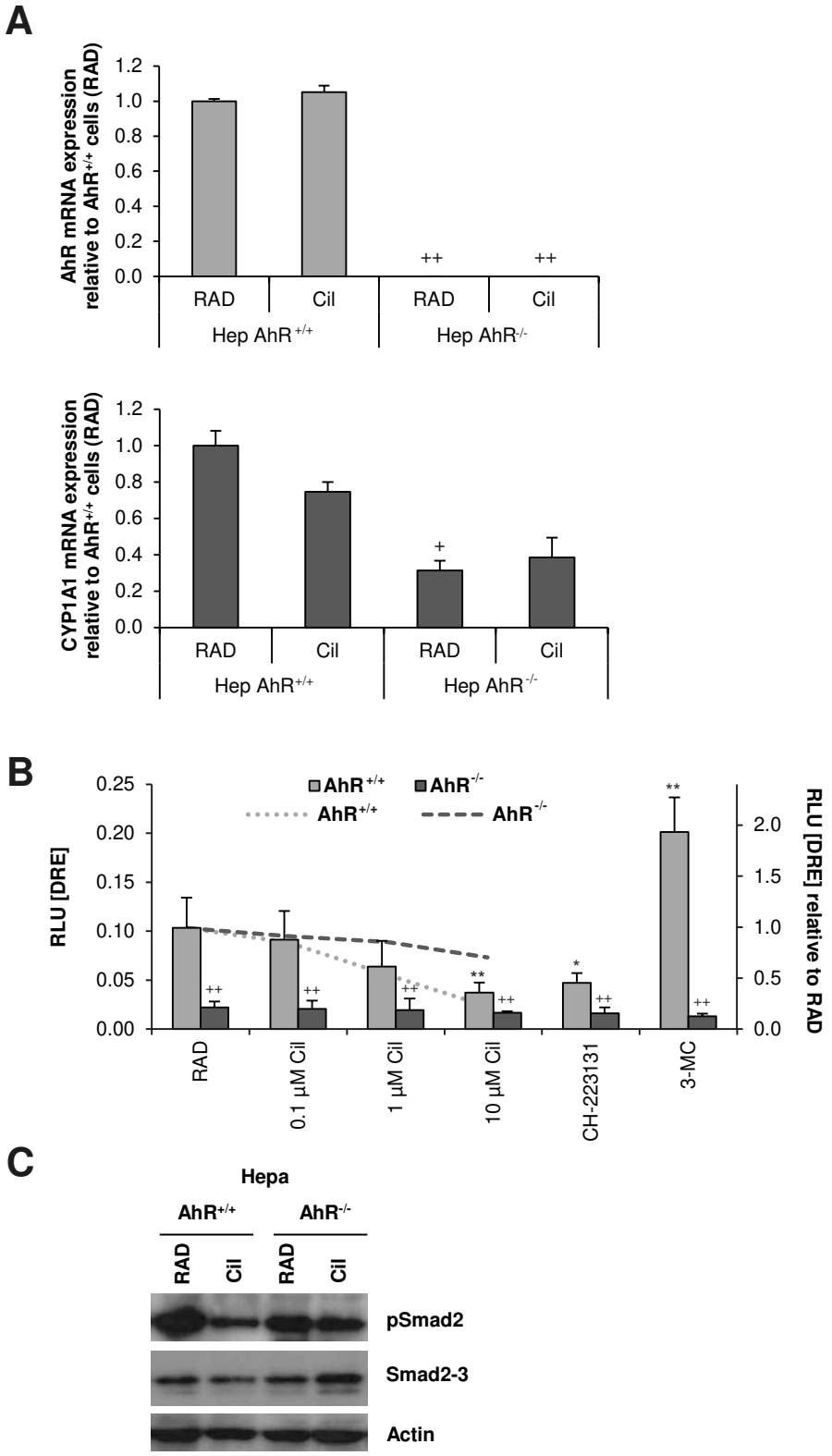
A
AhR mRNA expression relative to AhR+/+ cells (RAD)
1.2
1.0
0.8
0.6
0.4
0.2
0.0
++
++
RAD
Cil
RAD
Cil
Hep AhR+/+
Hep AhR-/-
CYP1A1 mRNA expression relative to AhR+/+ cells (RAD)
1.2
1.0
0.8
0.6
0.4
0.2
0.0
+
RAD
Cil
RAD
Cil
Hep AhR+/+
Hep AhR-/-
B
AhR+/+
AhR-/-
AhR+/+
AhR-/-
RLU [DRE]
RLU [DRE] relative to RAD
0.25
0.20
0.15
0.10
0.05
0.00
2.0
1.5
1.0
0.5
0.0
**
*
**
++
RAD
0.1 µM Cil
1 µM Cil
10 µM Cil
CH-223131
3-MC
C
Hepa
AhR+/+
AhR-/-
RAD
Cil
RAD
Cil
pSmad2
Smad2-3
Actin

Fig. 5

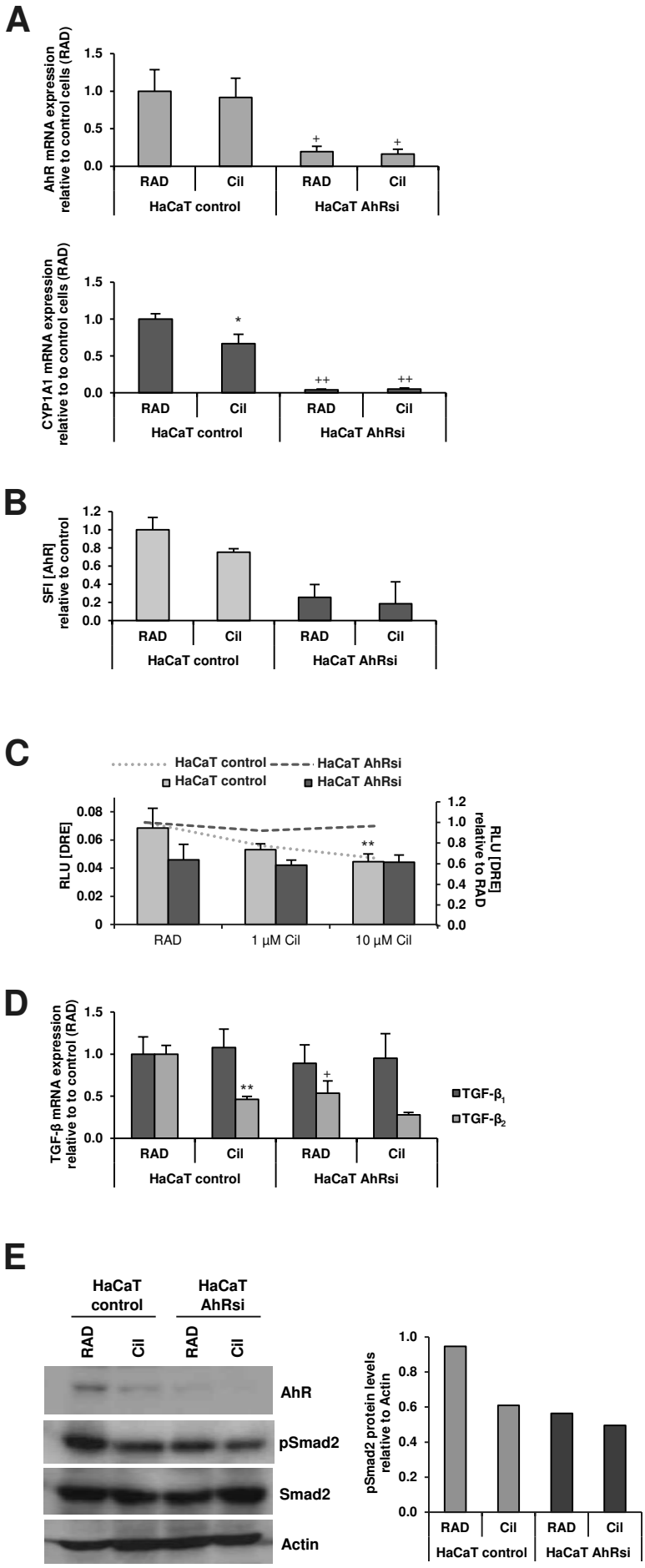
A
AhR mRNA expression relative to control cells (RAD)
1.5
1.0
0.5
0.0
+
+
RAD
Cil
RAD
Cil
HaCaT control
HaCaT AhRsi
CYP1A1 mRNA expression relative to to control cells (RAD)
1.5
1.0
0.5
0.0
*
++
++
RAD
Cil
RAD
Cil
HaCaT control
HaCaT AhRsi
B
SFI [AhR] relative to control
1.2
1.0
0.8
0.6
0.4
0.2
0.0
RAD
Cil
RAD
Cil
HaCaT control
HaCaT AhRsi
C
HaCaT control
HaCaT AhRsi
HaCaT control
HaCaT AhRsi
RLU [DRE]
0.08
0.06
0.04
0.02
0
RLU [DRE] relative to RAD
1.2
1.0
0.8
0.6
0.4
0.2
0.0
**
RAD
1 µM Cil
10 µM Cil
D
TGF-β mRNA expression relative to to control (RAD)
1.5
1.0
0.5
0.0
**
+
TGF-β1
TGF-β2
RAD
Cil
RAD
Cil
HaCaT control
HaCaT AhRsi
E
HaCaT control
HaCaT AhRsi
RAD
Cil
RAD
Cil
AhR
pSmad2
Smad2
Actin
pSmad2 protein levels relative to Actin
1.0
0.8
0.6
0.4
0.2
0.0
RAD
Cil
RAD
Cil
HaCaT control
HaCaT AhRsi

Fig. 6

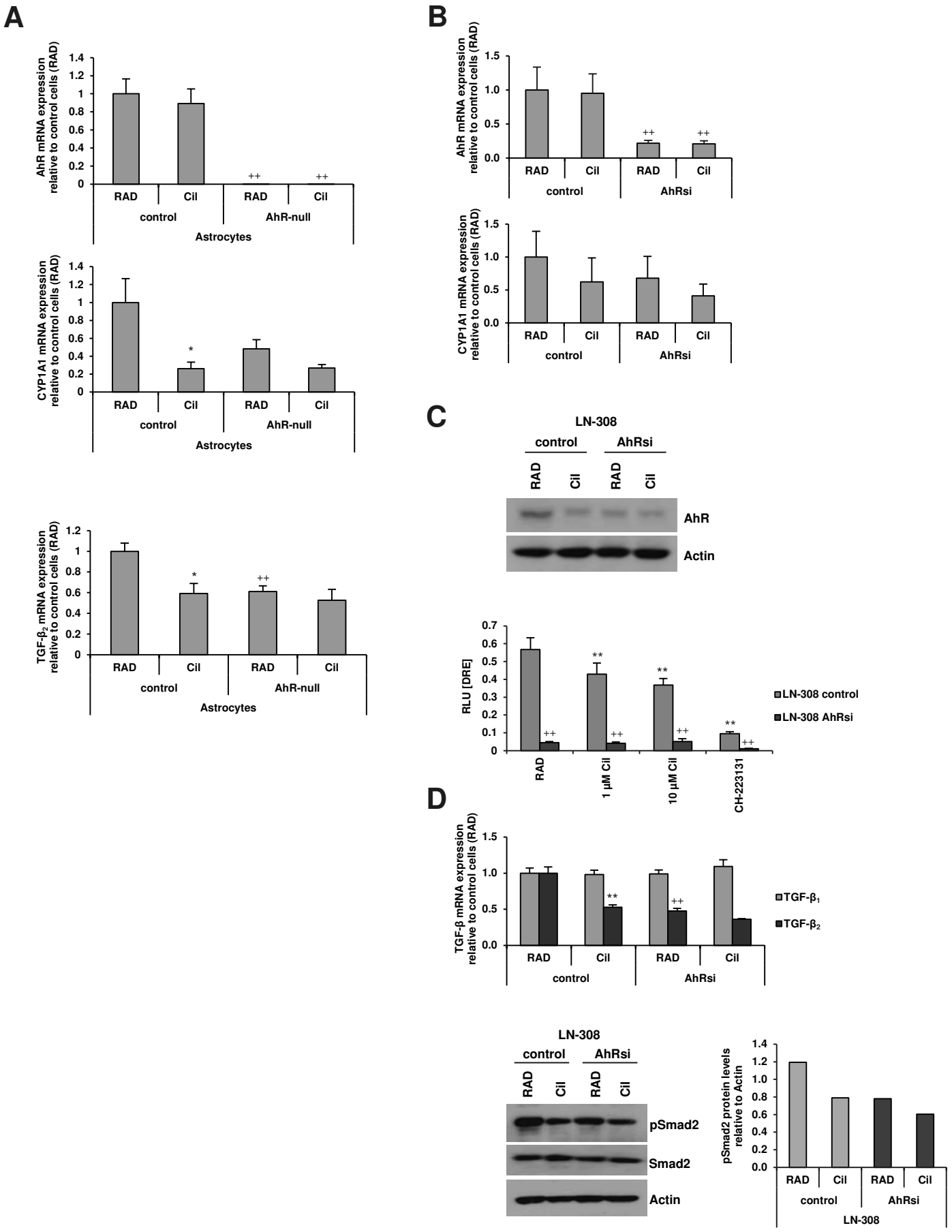
A
AhR mRNA expression relative to control cells (RAD)
CYP1A1 mRNA expression relative to control cells (RAD)
TGF-β2 mRNA expression relative to control cells (RAD)
RAD
Cil
control
AhR-null
Astrocytes
B
AhR mRNA expression relative to control cells (RAD)
CYP1A1 mRNA expression relative to control cells (RAD)
AhRsi
C
LN-308
AhR
Actin
RLU [DRE]
LN-308 control
LN-308 AhRsi
1 μM Cil
10 μM Cil
CH-223131
D
TGF-β mRNA expression relative to control cells (RAD)
TGF-β1
TGF-β2
pSmad2
Smad2
pSmad2 protein levels relative to Actin

Fig. 7

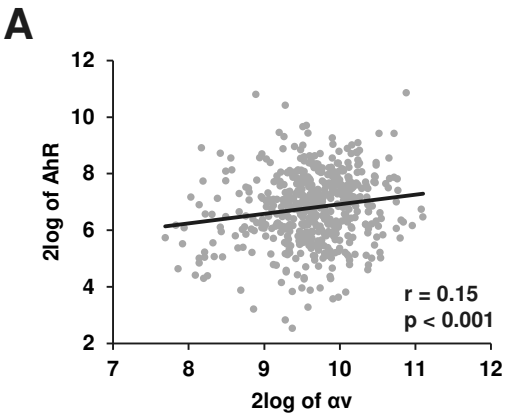
A
2log of AhR
2log of αv
r = 0.15
p < 0.001

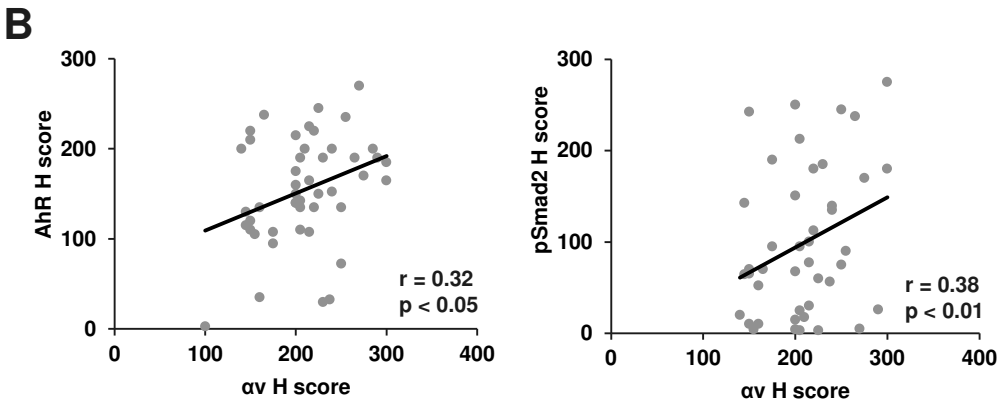
B
AhR H score
αv H score
r = 0.32
p < 0.05
pSmad2 H score
αv H score
r = 0.38
p < 0.01

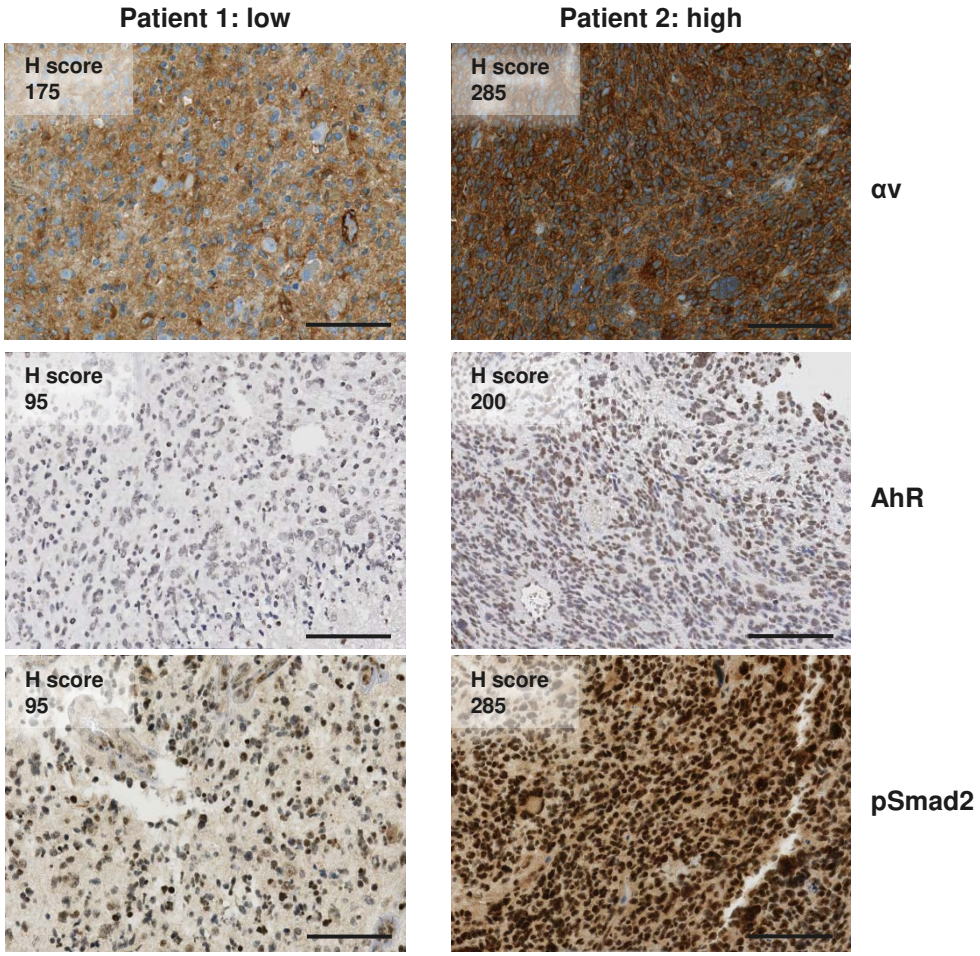
Patient 1: low
Patient 2: high
H score 175
H score 285
αv
H score 95
H score 200
AhR
H score 95
H score 285
pSmad2